Electronic Supplementary Material (ESI) for Environmental Science: Nano.

SUPPORTING INFORMATION

Biodegradation of graphene oxide-polymer nanocomposite films in wastewater

Jingjing Fan[1], Carlos David Grande[2], Debora F. Rodrigues[1]*

[1] Department of Civil and Department of Environmental Engineering, University of Houston, Houston, TX 77204-5003, dfrigirodrigues@uh.edu

[2] Department of Chemistry, Universidad del Atlántico, Puerto Colombia, Atlantico 8000-1 , Colombia

2.1. Materials

All the chemicals were obtained from Sigma-Aldrich unless stated otherwise. Chitosan (CS) was obtained from Sigma-Aldrich (degree of deacetylation: 85%, Mw = 190,000-310,000 Da). Graphite flakes were purchased from XG sciences Ltd. and were used to prepare graphene oxide. Phosphate buffer solution (PBS, 0.01 M, pH =7.4) used for microbial analysis was purchased from Fisher Scientific Inc. All the chemicals were used as received without any further purification.

2.2. Graphene oxide preparation.

The synthesis of GO was carried out following the procedure previously reported by our research group: Briefly, three grams of graphite flakes and 400 mL of concentrated H_2SO_4 were mixed in a 2000 mL round bottom flask. Then, 3.0 g of $KMnO_4$ was slowly added to the reaction mixture, which immediately turned dark green. Three more 3.0 g portions of $KMnO_4$ were added to the reaction mixture every 24 h. The reaction was stopped after 4 day of reaction period in an ice-water bath mixture. After which, H_2O_2 was slowly added turning the dark purple solution to yellow. Solids were separated from the solution by centrifugation and the supernatant was discarded, while the settled nanomaterial was washed with Milli-Q water and isopropanol until constant pH was achieved. The nanomaterial was then sieved using No. 80 and No. 100 USA Standard Testing Sieve. The sieved nanomaterial was dialyzed for three days in isopropanol using 3.5K MWCO dialysis tube. The graphite oxide solids were obtained by vacuum evaporation. To obtain GO, the graphite oxide solution was sonicated for 30 minutes (Cole Palmer Ultrasonic Processor, Model CV334).

2.3. Nanocomposite film preparation

Chitosan-graphene oxide nanocomposite films (CS-GO) were prepared according to a modified procedure previously described. Briefly, chitosan was dissolved in an aqueous solution (1% v/v) of glacial acetic acid to a concentration of 2% (w/v) by magnetic stirring. The solution was stirred at 40^{o}C using a disperser (IKA Ultraturrax T25) and was filtered through a Whatman No. 3 filter paper to obtain a clear solution. GO was dispersed into 1% acetic acid aqueous solution. The chitosan was added into the GO suspension, stirred for 1 h to form a homogeneous solution using the ultraturrax. The CS-GO solution was sonicated at 60°C for about 1 h, followed by pouring the CS-GO solution onto a glass plate for pre-reaction. After drying, CS-GO nanocomposite films were peeled off and further dried at 120°C overnight under vacuum for thermal post cross-linking. By changing the weight ratio of chitosan to graphene oxide, films with different GO loadings (0.25, and 0.6 wt %) were prepared (coded as CS-GO-0.25, and CS-GO-0.6).

2.4. Physicochemical and mechanical properties of the films

Thickness, thermal analysis and surface properties of the CS-GO nanocomposite films were determined. The means and standard deviations were calculated for all replicate samples and measurements. Film thickness was determined using a digital Mitutoyo Digimatic micrometer (coolant proof micrometer ip65) to the nearest 0.001 mm.

The gel content of the CS-GO films was calculated from equation (1) using dried slices of 2 cm^2 obtained after 12 h contact with water and dried to constant weight in oven at 40°C.

$$[\text{Gel content } (\%) = (W_f/W_i) \times 100] \qquad \text{Equation (1)}$$

Where W_f is the final weight of the film obtained after drying in oven at 40°C and W_i is the initial weight of the film prior to contact with water.

Thermal properties of the polymers were measured by thermal gravimetric analysis (TGA) on a TA Instruments TGA 2920. The samples were heated up to 900 °C at a heating rate of 10°C/min under dry nitrogen atmosphere (flow rate 80 mL/min). The glass transition temperature (Tg) was determined by differential scanning calorimetry (DSC) from the midpoint of the inflection tangent from the second heating at 10°C/min. TGA and DSC data were analyzed using TA Instruments' Universal Analysis software.

The mechanical characterization was performed on a mechanical analyzer (Shimadzu EZ-LX, Japan). Each film was cut into three dumbbell strips with a size of 165 mm × 20 mm, to obtain a test size 125mm x 22mm. The lower grip was fixed and the upper grip rose at an extension rate of 12 mm/min with a preload of 1.0 N. All the failures occurred at the middle region of the testing strips. The mechanical characterization of chitosan films was performed according to the ASTM D882–12.

2.5 Contact angle measurement

Water contact angle measurement was used to evaluate the hydrophobicity of the nanocomposite surfaces. CS-GO films surfaces were characterized by water contact angle through the sessile drop method [1]. Briefly, the sample was secured in a sample holder and placed on a stage illuminated for camera viewing. A deionized water droplet (3-5 µL) was placed on the surface. The images of the drop on the surface were taken by camera and then imported into ImageJ. The static contact angles were measured using Image J LB-ADSA plugin. For each measurement, two points were chosen to manually define the baseline and three points along the drop profile. The program then fits the profile of the drop to calculate the contact angle using the sphere approximation, or the ellipse approximation. Measurements of contact angle for each sample were carried out in triplicate. For samples showing varying results, up to five measurements were performed.

2.6. Detection of Superoxide Radical Anion (•O_2^-)

The mechanism of anti-microbial activity of CS-GO nanocomposites was investigated through radical related oxidative stress. To determine the production of superoxide radical anion (•O_2^-), the XTT (2,3- bis(2-methoxy-4-nitro-5 sulfophenyl)-2H-tetrazolium-5-carboxanilide, Biotium) assay was performed. The XTT can be reduced by superoxide radical anion (•O_2^-) to form the water soluble XTT-formazan that has maximum absorption at 470 nm. Briefly, 25 µl of the activation reagent (5 mM phenazine methosulfate (PMS)) and 5 ml of the XTT solution (1mg/ml) were mixed in the dark to activate the XTT solution. A volume of 5 mL of freshly prepared activated XTT solution was added to the 6 well plates (Costar 3370, Corning, NY) with the CS-GO films. The mixture was incubated 3 h for reaction. After incubation, the liquid solution was filtered through 0.2 µm PTFE membrane filters (Millipore), and then 100 µL filtered solution was placed in a 96-well plate (Corning Inc.,USA). The change in absorbance at 470 nm was monitored by the plate reader method (EL800 universal microplate reader; Bio-Tek Instruments, Inc., Winooske, VT). In this assay, 50 ppm of TiO_2 dispersion exposed to UV light served as positive control, while the pure chitosan film was used as negative control. All experiments were done in triplicates and the results were averaged. Standard deviations were calculated based on the triplicate experiments.

3.1 CS-GO Films Characterization

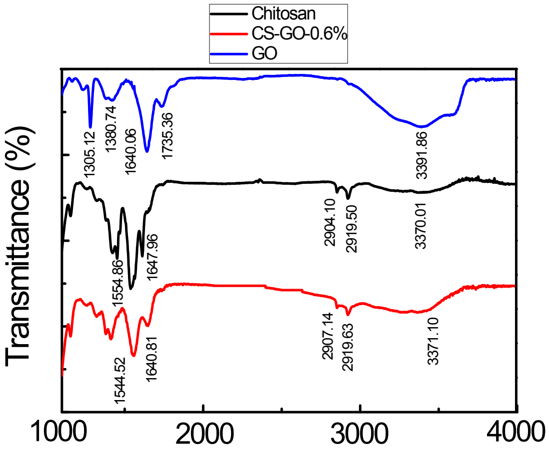

Figure S1: FTIR analysis for chitosan, GO, and CS-GO-0.6% nanocomposite after synthesis.

FTIR was carried out to verify the functional groups of GO, chitosan and CS-GO nanocomposites. Since CS-GO-0.6% contained the highest amount of GO compared to other films, we are presenting the results of 0.6% as a representative data since the other films presented similar patterns. As shown in Figure 1, in the spectrum of GO, the dominant peaks were at 1305, 1380, 1640, 1735 and 3391 cm^{-1}. The peak at 1305 cm^{-1} corresponds to a stretching vibration from C-O-C bonds of epoxy. The peak at 1380 cm^{-1} is attributed to the C-OH bonds, while the peak centered at 1640 cm^{-1} is assigned to C=C bonds associated with skeletal vibrations of unoxidized graphite domains. The peaks located at 1820 cm^{-1} and 3391 cm^{-1} are attributed to C=O in carboxylic acid and O-H stretching vibration, respectively. Other studies also confirmed that these characteristic functional groups in GO make it highly hydrophilic and dispersible [2]. In the spectrum of chitosan, there are two characteristic absorbance bands centered at 1554 cm^{-1} and 1647 cm^{-1}, which correspond to the C-O stretch vibration of –NHCO- (amide I) and the N-H bending of –NH_2, respectively [3]. The peak at 1378 cm^{-1} was attributed to the characteristic band of the CH_3 function. A broadband at around 3370 cm^{-1} was assigned to –NH stretching. In the spectrum of CS-GO-0.6%, the dominant peak of chitosan at 1554 cm^{-1} shifted to 1536 cm^{-1}. This change corresponds to the stretching vibration from C=O of -NHCO- and the N-H bending of NH_2, which happens when there is an epoxy-amine reaction [4]. The increased intensity of the nanocomposite peak at 3371 cm^{-1} comparing to pure chitosan suggested that amine stretching from chitosan and –OH groups of GO were involved in the nanocomposite formation [5]. However, the peak at 1820 cm^{-1} which corresponding to C=O in carboxylic acid of GO is absent in CS-GO-0.6% spectrum. This could be due to the low mass ratio of GO in the chitosan (0.6%) matrix of the nanocomposite.

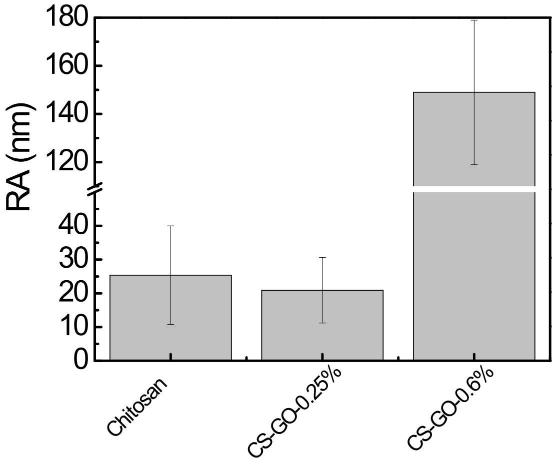

Figure S2: AFM analysis of CS-GO with different GO content as synthesized.

To quantitatively investigate the surface topography of the CS-GO nanocomposites, AFM was used to investigate the surface morphology of the films. The surface roughness parameter is average roughness (R_a), which showed the effect of GO addition on the matrix of the chitosan (Figure 2). As can be seen, the R_a of CS-GO films didn't show a significant difference at low GO concentration (0.25%) comparing to pure chitosan. However, R_a significantly increased on the CS-GO-0.6%. This can be attributed to some GO sheets protruding from the film and making it rougher [6]. It is also worth noting that GO sheets exist with very sharp edges and flat surfaces. Thus, the appearance of the edges of GO which generated from the polymer wrapping and folding could cause the relative coarse surface of CS-GO nanocomposites. The similar phenomenon has been widely observed in recent studies [7, 8]. Another possible contribution to the high roughness could be the crumpling of the graphene oxide nanoplates [9].

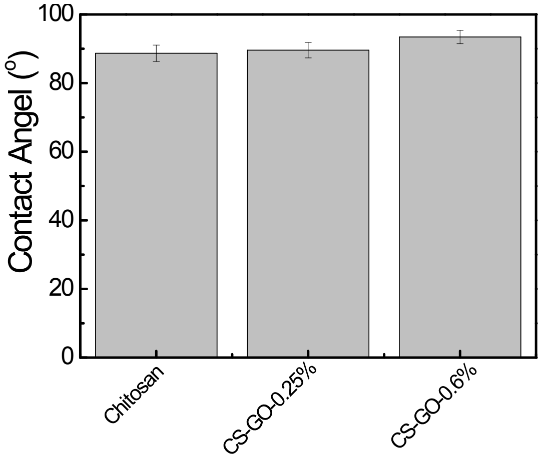

Figure S3: Contact angle measurements for CS-GO nanocomposites with different GO content prior to experiments with wastewater.

The hydrophobicity of CS-GO nanocomposites was investigated using contact angle measurements. According to the widely accepted relationship between the contact angle and hydrophobicity, the contact angle for pure chitosan nanocomposite film suggested that it behaved as a hydrophobic polymer ($\theta \approx 90^{o}$). This value is in agreement with values reported by others [10, 11]. Some researchers proposed that dispersing GO into the chitosan matrix could have made the nanocomposites more hydrophilic due to the introduction of -OH functional groups [12]. In the present study, the hydrophobicity change was not observed with the concentrations used of GO. The possible reason could be the low content of GO, since other studies normally start to visualize the change in hydrophobicity in nanocomposites containing 2% GO. [12, 13].

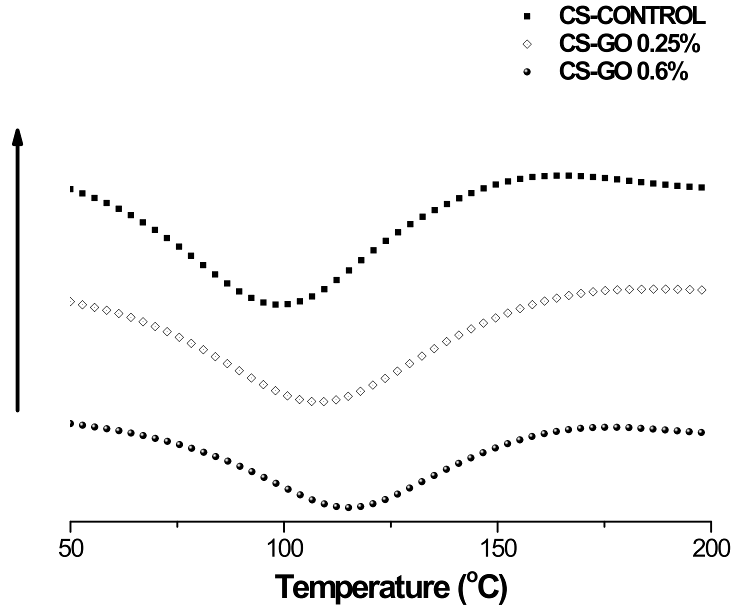

Figure S4: DSC plot for different CS-G0 nanocomposite films as synthesized.

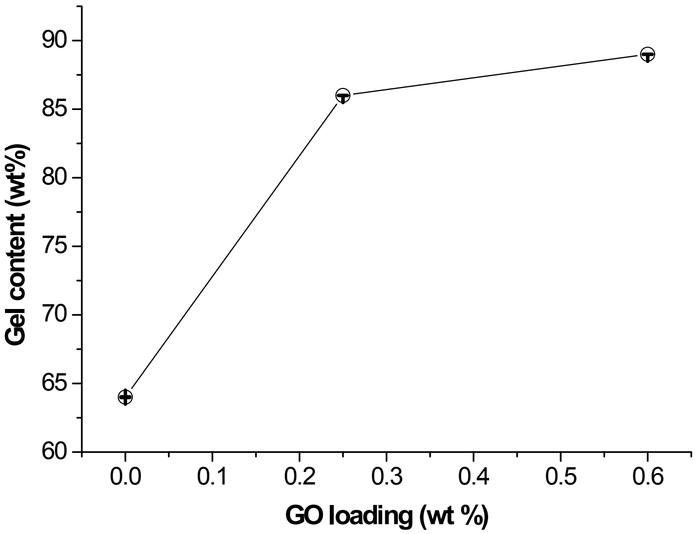

Figure S5: Gel content results for CS-GO nanocomposites with different GO loadings.

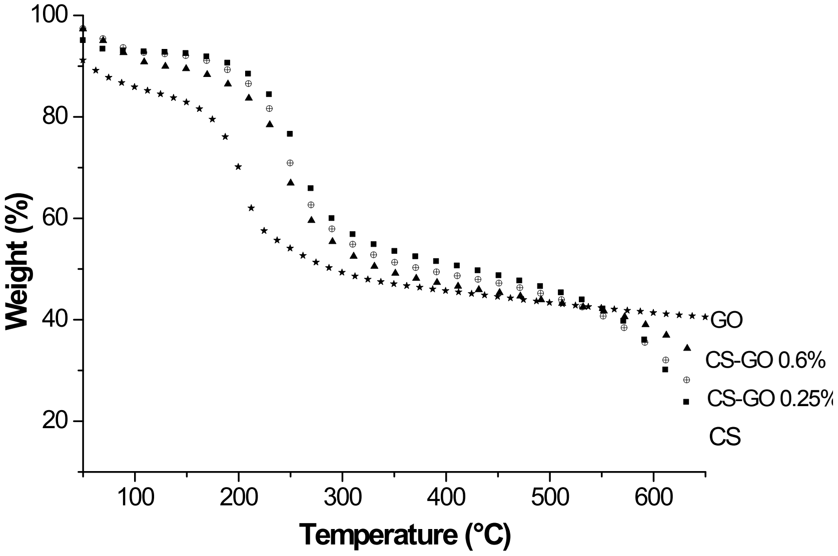

Figure S6: TGA results for CS-GO nanocomposites before experimentation with sludge.

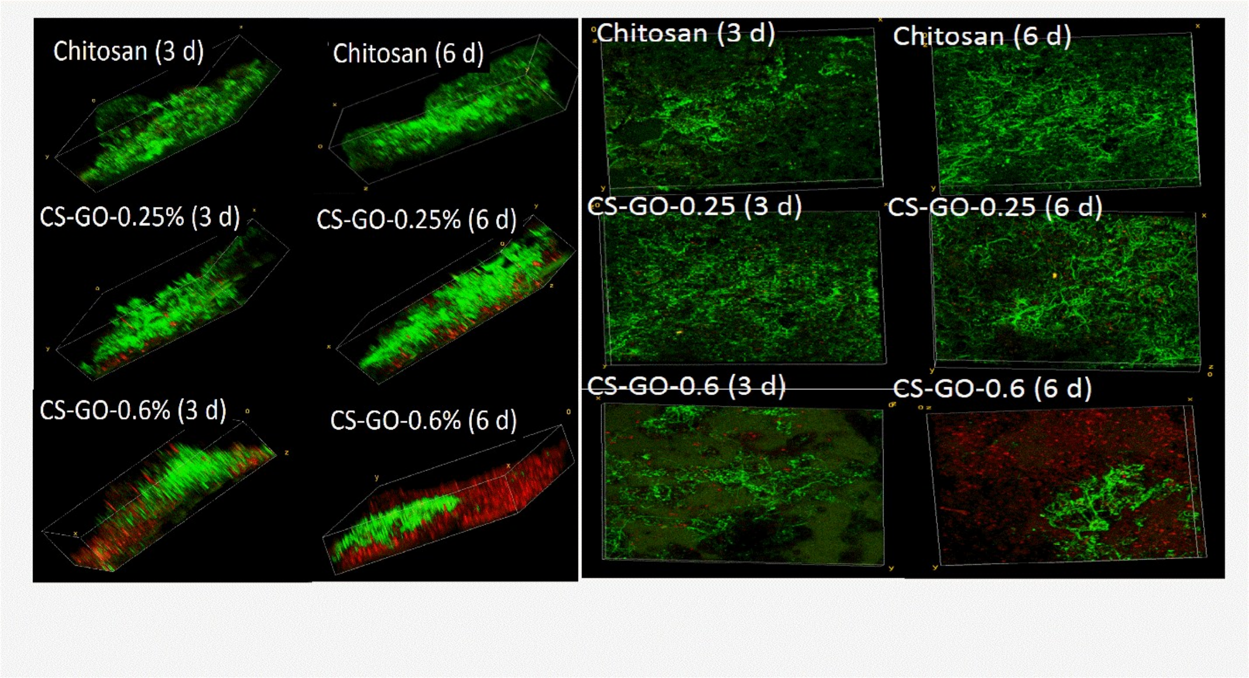

Figure S7: The CLSM analysis of biofilm for CS, CS-GO-0.25%, and CS-GO-0.6% films. The left images correspond side view of the biofilms, while the right images are bottom view of all biofilms.

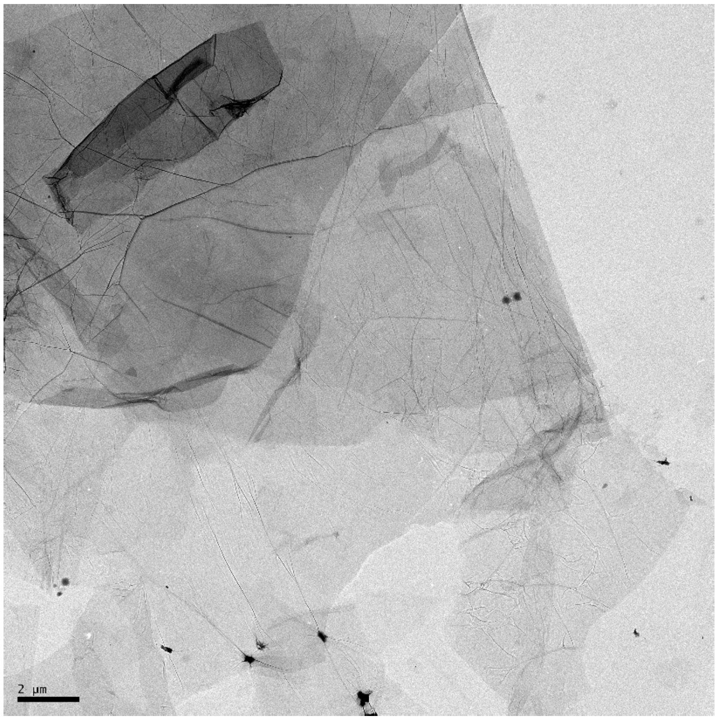

Figure S8: TEM image for GO particle size

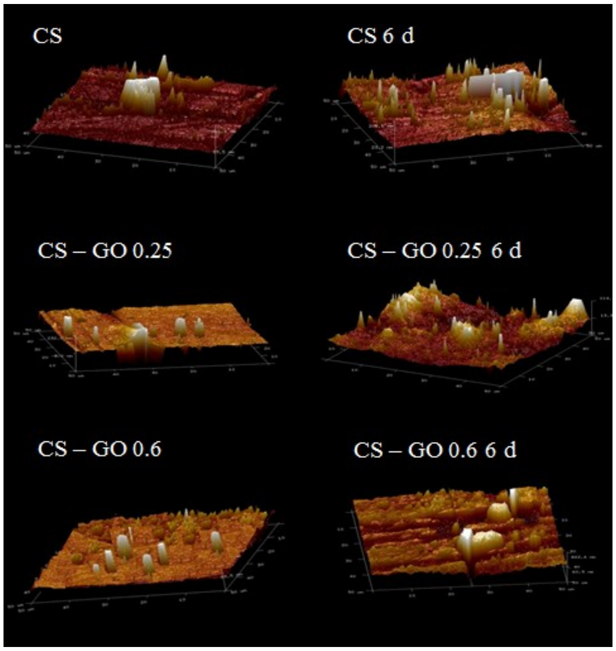

Figure S9: AFM images for surface roughness

References:

1. Y. Rotenberg, L. Boruvka and A. Neumann, *Journal of colloid and interface science*, 1983, **93**, 169-183.
2. X. Yang, Y. Tu, L. Li, S. Shang and X.-m. Tao, *ACS Applied Materials & Interfaces*, 2010, **2**, 1707-1713.
3. M. Ibrahim, O. Osman and A. A. Mahmoud, *Journal of Computational and Theoretical Nanoscience*, 2011, **8**, 117-123.
4. L. Shao, X. Chang, Y. Zhang, Y. Huang, Y. Yao and Z. Guo, *Applied Surface Science*, 2013, **280**, 989-992.
5. K. Sundar, V. Harikarthick, V. S. Karthika and A. Ravindran, *Journal of Bionanoscience*, 2014, **8**, 207-212.
6. M. Mazaheri, O. Akhavan and A. Simchi, *Applied Surface Science*, 2014, **301**, 456-462.
7. J. Shen, Y. Hu, C. Li, C. Qin and M. Ye, *small*, 2009, **5**, 82-85.
8. M. Fang, K. Wang, H. Lu, Y. Yang and S. Nutt, *Journal of Materials Chemistry*, 2009, **19**, 7098-7105.
9. H. Bao, Y. Pan, Y. Ping, N. G. Sahoo, T. Wu, L. Li, J. Li and L. H. Gan, *Small*, 2011, **7**, 1569-1578.
10. S. Farris, L. Introzzi, P. Biagioni, T. Holz, A. Schiraldi and L. Piergiovanni, *Langmuir*, 2011, **27**, 7563-7574.
11. J. Desbrieres, C. Martinez and M. Rinaudo, *International journal of biological macromolecules*, 1996, **19**, 21-28.
12. A. Ammar, A. M. Al-Enizi, M. A. AlMaadeed and A. Karim, *Arabian Journal of Chemistry*, 2016, **9**, 274-286.
13. M. Yadav, K. Y. Rhee and S. J. Park, *Carbohydrate Polymers*, 2014, **110**, 18-25.